

**ADSORPTION PHYSICS OF METALS PARTIALLY COVERED BY
METALLIC PARTICLES. PART III:
EQUATIONS OF STATE AND ELECTRON EMISSION S-CURVES**

J. D. LEVINE* and E. P. GYFTOPOULOS

*Department of Nuclear Engineering and Research Laboratory of Electronics,
Massachusetts Institute of Technology, Cambridge, Mass., USA.*

Received 29 June 1964

Surface equations of state and electron emission S -curves for metallic surfaces immersed in monatomic metallic vapors are calculated theoretically. The results are shown to be in agreement with most of the available experimental results. No adjustable parameters are used.

1. Introduction

In previous studies the theoretical calculations of electron work function¹), atom and ion desorption energies²), and desorption rates³) for bimetallic adsorption systems were reported. In this communication the results of these studies are combined to establish the equations of state that relate the degree of coverage θ to the temperatures, T of the surface and T' of the vapor bath, and to the sheath potential, ϕ_s , prevailing in the vicinity of the surface. Such equations are useful both for studies of surface hysteresis effects and for the derivation of electron emission S -curves.

Many relations $\theta(T, T')$ have been reported by others, usually in the form of isotherms and they are reviewed by de Boer⁴) and Emmett⁵). These isotherms, however, do not account for the nonlinear variation of the desorption energy with θ , and many of the parameters are adjustable.

Calculations of electron emission S -curves have also been derived by other authors either by means of a perturbation technique⁶) of the Taylor-Langmuir⁷) cesium-tungsten system or by considering the initial adsorption energy as an adjustable parameter⁸).

2. Surface equation of state

The purpose of this section is to derive an equation of state for metallic

* Present Address: RCA Research Laboratories, Princeton, N.J., U.S.A.

surfaces partially covered by monatomic metallic particles, including the effect of a positive sheath potential, ϕ_x , in the vicinity of the surface. The adsorption system under consideration is defined in ref.³) apart from the sheath potential which is introduced for the purposes of the present discussion.

The general equation of state is a balance between incoming and unreflected outgoing particles. Specifically:

$$E' = E_a + E_p \exp(-\phi_x/kT) \quad (1)$$

where $E' = \omega_a v' \sigma' \exp(-\phi'/kT')$ = rate of atom arrival from vapor bath*, $E_a = \omega_a v \sigma_f \theta \exp(\Delta S/k) \exp(-\phi_a/kT)$ = rate of atom emission from surface, $E_p = \omega_p v \sigma_f \theta \exp(\Delta S/k) \exp(-\phi_p/kT)$ = rate of ion emission from surface, and all other quantities are defined and/or computed in ref.^{2,3}). From these definitions it is readily seen that the surface equation of state is an explicit or implicit function of fundamental properties of the materials involved in the adsorption system, the degree of surface coverage θ and the temperatures T and T' of the surface and the vapor bath, respectively.

In order to illustrate some of the implications of the equation of state, the right hand side of eq. (1) is depicted in fig. 1 as a function of θ . The figure is derived for the system cesium-tungsten with the crystallographically sensitive properties: bare tungsten electron work function $\phi_m = 4.62$ eV, electron work function at one monolayer coverage $\phi_f = 1.81$ eV, number of adatoms at one monolayer $\sigma_f = 4.8 \times 10^{14}$ cm⁻² and with other typical properties taken from table 1²) and table 2³). The surface temperature is $T = 1400^\circ$ K.

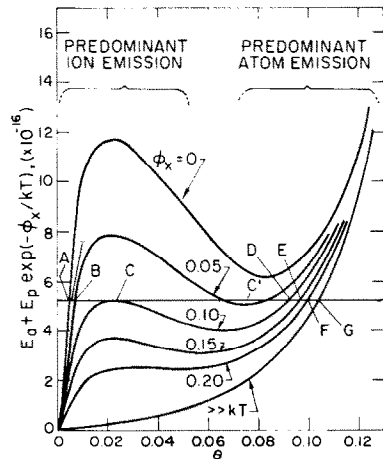


Fig. 1. Theoretical plot of atom plus ion desorption rates of cesium from tungsten versus coverage for different values of the sheath potential and $T = 1400^\circ$ K.

* If locally superheated vapor is present, then E' is decreased by the factor $\sqrt{T'/T}$, obtained from a pressure balance.

It is observed that when ϕ_x is of the order of kT and given an appropriate arrival rate E' (represented by a horizontal line in fig. 1), surface state equilibrium occurs for several values of θ . This multivaluedness of θ leads to new hysteresis effects as illustrated in fig. 2 where θ , E_p and the electron emission rate $I_e = 120T^2 \exp(-\phi_e/kT)$ are plotted versus ϕ_x for $T' = 366^\circ\text{K}$.

Further analysis shows that given a value of the surface temperature, hysteresis effects occur only over a limited range of T' . For example, for the

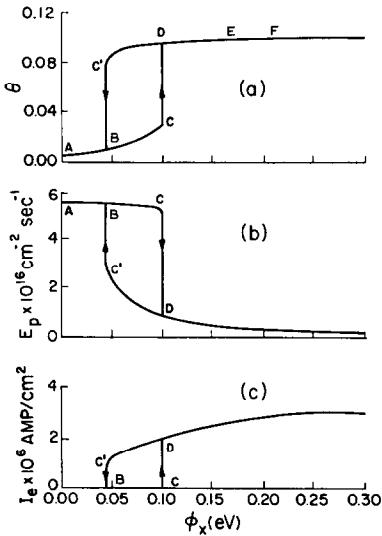


Fig. 2. Theoretical hysteresis effects in the system cesium-tungsten for $T = 1400^\circ\text{K}$, $T' = 366^\circ\text{K}$: (a) coverage; (b) ion emission; (c) electron emission versus sheath potential.

above system and $T = 1400^\circ\text{K}$, this range is $354^\circ\text{K} < T' < 368^\circ\text{K}$. For $T > 2000^\circ\text{K}$ there are no hysteresis effects because the variation of $E_a + E_p \exp(-\phi_x/kT)$ as a function of θ is monotonic.

Different hysteresis effects have been examined⁹⁻¹¹) previously under the conditions: $\phi_x = 0$, T' fixed, and T variable. The hysteresis occurs at low coverage, is reproducible, and has been observed for cesium on W, Re, Mo, and Nb. Indeed, a simple equation for the minimum temperature for saturated ion emission can easily be derived¹⁰) by maximizing E_p with respect to θ at constant T and setting the result equal to E' . It is necessary only to presume that the ion desorption energy increases linearly with θ for $\theta < 0.1$.

An important simplification of the equation of state occurs when $\phi_x \gg kT$. Then all the emitted ions are reflected back to the surface and all the emitted electrons are transmitted. Thus eq. (1) reduces to the form:

$$\frac{1000}{T} = \frac{\phi'_a}{\phi_a} \frac{1000}{T'} + \frac{1}{5.05\phi_a} \ln \left[\frac{v\sigma_f}{v'\sigma'} \exp(\Delta S/k) \right]. \quad (2)$$

Since the atom desorption energy, ϕ_a , the change in configuration entropy, ΔS , and the vibration frequency, ν , are functions of θ only, as shown in ref.^{2,3}, eq. (2) indicates that the coverage θ is a simple function of reciprocal T and T' .

A plot of eq. (2) for the same cesium-tungsten system, with θ as a free parameter, is shown in fig. 3. The region of values of interest is bounded by the vertical line, $1000/T = 0.27$, characteristic of melting tungsten and by the 45° line, $T = T'$, corresponding to bulk liquid cesium formation. The dashed 45° line indicates the calculated region in which the formation of the second layer becomes important³). The melting transition of bulk cesium introduces a small slope change of the isotheric lines at the melting point $1000/T' = 3.3$.

Superimposed on fig. 3 are also experimental data reported by Taylor and Langmuir⁷) who specified that for their cesium on tungsten system $\phi_m = 4.62\text{eV}$, $\phi_f = 1.81\text{eV}$, $\sigma_f = 4.8 \times 10^{14}\text{cm}^{-2}$. The agreement between theory and experiment is good. No adjustable parameters are used.

The quasi-linear relationship between $1/T$ and $1/T'$ for constant θ , under conditions of saturated electron emission, has also been derived by other authors who did not, however, give explicit formulas for the calculation of the slopes and intercepts of the isotheric lines^{6,12}).

Plots similar to those of fig. 3 can be constructed for other adsorption systems but the reported experimental data are not adequately described to permit meaningful quantitative comparisons. Qualitatively, experimental

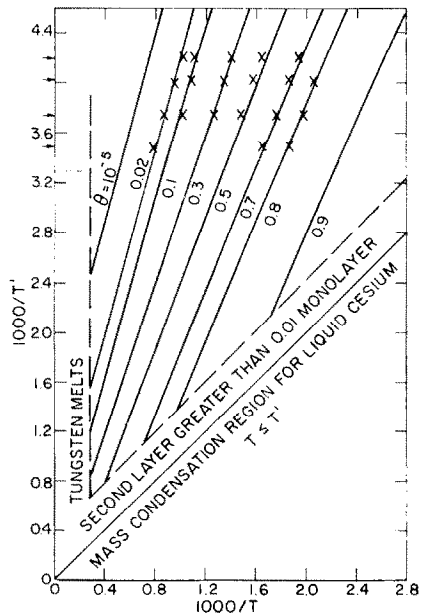


Fig. 3. Comparison of theoretical surface equation of state (solid lines) with experimental results (crosses) for tungsten coated by cesium when $\phi_x \gg kT$.

results of constant electron work function ϕ_e plotted on a $1/T$ versus $1/T'$ plane fall on a straight line¹³). In addition, for $0.1 < \theta < 0.4$, ϕ_e is approximately a unique function⁶) of T/T' . These results are in agreement with the present theory.

3. Electron emission S-curves

The purposes of this section are to theoretically derive electron emission *S*-curves for bimetallic adsorption systems, to discuss the sensitivity of these curves with respect to various characteristic parameters of the system, and to compare the derived results with available experimental data.

Electron emission *S*-curves are plots of saturated, field free electron emission versus $1000/T$ with T' as a running parameter. They are derived by combining the Richardson equation

$$I_e = 120T^2 \exp(-\phi_e/kT) \quad (3)$$

with the equation of state (eq. (2)).

The derivation of *S*-curved involved some ambiguity with regard to the appropriate value of the sheath potential, ϕ_x , that must be used in eq. (1). Specifically for $\phi_x \gg kT$ the electron emission is saturated but not strictly field free. On the other hand, for $\phi_x \simeq 0$, the electron emission is field free but not truly saturated when the reflected ions can alter the coverage (fig. 2c).

For the purposes of discussing saturated electron emission, ϕ_x is taken much greater than kT but not large enough to result in appreciable field emission. This choice is consistent with the way saturated measurements were made by different experimenters^{7, 14, 15}). Zollweg¹⁶) proposes that *S*-curves correspond to $\phi_x = 0$, but this is not in accord with experimental conditions since all measurements are taken with a positive potential of the order of a volt.

3.1 SENSITIVITY OF S-CURVES

The family of *S*-curves of fig. 4 are calculated for a hypothetical cesium-tungsten system with $T' = 473^\circ\text{K}$. Curve *A* is derived for $\phi_m = 4.62\text{eV}$, $\phi_f = 1.81\text{eV}$, $\sigma_f = 4.8 \times 10^{14}\text{cm}^{-2}$. Curves *B* through *F* are derived by arbitrarily varying ϕ_m , ϕ_f and σ_f by $\pm 10\%$ and using different combinations of these values as shown in the figure.

The main conclusion from this figure is: if for different crystallographic arrangements of the substrate 10% independent variations of ϕ_m , ϕ_f , σ_f are possible, then the electron emission may vary by an order of magnitude. This conclusion is general because it applies to other adsorbate-substrate combinations besides cesium-tungsten. It has been verified qualitatively by many

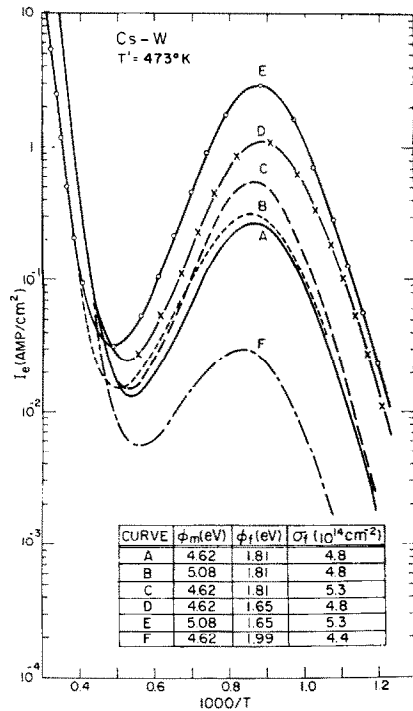


Fig. 4. Parametric study of sensitivity of S -curves for the system cesium-tungsten for different combinations of values of ϕ_m , ϕ_f , and σ_f and $T' = 473^\circ\text{K}$.

experimenters^{6,17,18}) and quantitatively by means of field emission measurements^{14,19}).

Another conclusion of this analysis is that small independent variations of ϕ_f , caused by epitaxial growth of the monolayer, are much more effective in causing higher electron emission than similar variations of ϕ_m and/or σ_f . The conclusion is in contrast to the currently accepted idea⁶) that S -curves are *exclusively* sensitive to ϕ_m . If this idea were true, then S -curves would not cross over in their rising parts (see curves B and C, fig. 4) which is contrary to experimental results^{14,17-19}). Admittedly, the contradiction might be reconciled by assuming that the variations of ϕ_m , ϕ_f and σ_f are coupled. At the present time, however, there is no known correlation between these quantities.

3.2. COMPARISON OF THEORY WITH EXPERIMENTAL RESULTS

The comparison of theoretical S -curves with reported experimental results is somewhat ambiguous because many experimenters do not specify the important parameters ϕ_m , ϕ_f and σ_f pertinent to their specimens. There are two alternatives to take in attempting to compare theory with these experi-

ments: (a) use typical values of ϕ_m , ϕ_f , and σ_f , with the uncertainty that they are not necessarily applicable to the data under consideration; (b) determine the set of ϕ_m , ϕ_f and σ_f values that best fit the data, but then the correlation is not truly theoretical. In what follows both alternatives are presented. Input parameters other than ϕ_m , ϕ_f , and σ_f are taken from table 1²⁾ and table 2³⁾.

3.2.1. *Cs on polycrystalline W*

Fig. 5 presents a family of *S*-curves for the system cesium-tungsten derived for $\phi_m = 4.62\text{eV}$, $\phi_f = 1.81\text{eV}$, $\sigma_f = 4.8 \times 10^{14}\text{cm}^{-2}$ and different cesium bath temperatures (solid lines).

Superimposed on the same figure are the *S*-curves reported by Taylor and Langmuir⁷⁾ for $T' = 237^\circ\text{K}$, 270°K and 313°K (dashed lines). These authors reported that their specimens had $\phi_m = 4.62\text{eV}$, $\phi_f \cong 1.81\text{eV}$ and $\sigma_f = 4.8 \times 10^{14}\text{cm}^{-2}$. Good agreement between theory and experiment is observed over several orders of magnitude. The agreement would improve substantially if the theoretical curves were derived for $\phi_m = 4.62\text{eV}$, $\phi_f = 1.75\text{eV}$ and $\sigma_f = 4.8 \times 10^{14}\text{cm}^{-2}$.

Houston¹⁴⁾ reported *S*-curves for cesium on a different specimen of tungsten and $T' = 373^\circ\text{K}$, 423°K , 473°K , $\phi_m = 4.62\text{eV}$. His data are also shown in fig. 5 (circles). The agreement with the theoretical curves is favorable but it is better if $\phi_m = 4.62\text{eV}$, $\phi_f = 1.65\text{eV}$, $\sigma_f = 4.5 \times 10^{14}\text{cm}^{-2}$.

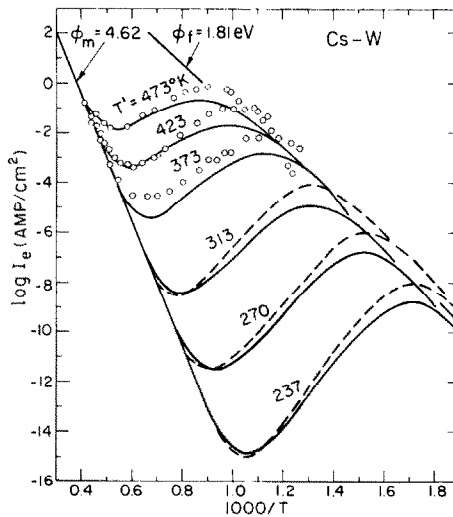


Fig. 5. Comparison of theoretical *S*-curves (solid lines) with experimental results of Taylor and Langmuir (dashed lines) and Houston (circles) for the system cesium-tungsten.

3.2.2. Cs on polycrystalline Mo

Fig. 6 presents a family of S-curves for cesium on polycrystalline molybdenum derived for $\phi_m = 4.38\text{eV}$, $\phi_f = 1.81\text{eV}$ and $\sigma_f = 4.8 \times 10^{14}\text{cm}^{-2}$. Superimposed on the figure are also the data of Houston¹⁴⁾ and Aamodt *et al.*¹⁵⁾ for similar systems. The agreement between theory and experiment

Fig. 6. Comparison of theoretical S-curves (solid lines) with experimental results of Houston (triangles) and Aamodt *et al* (circles and squares) for the system cesium-molybdenum.

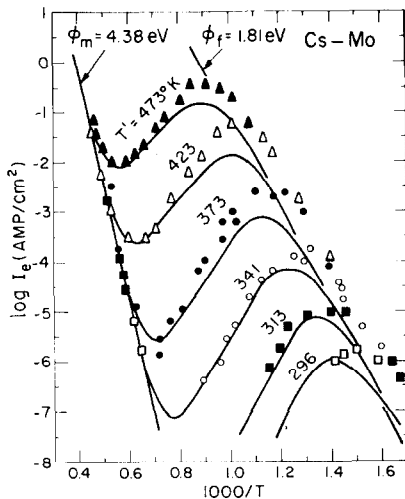
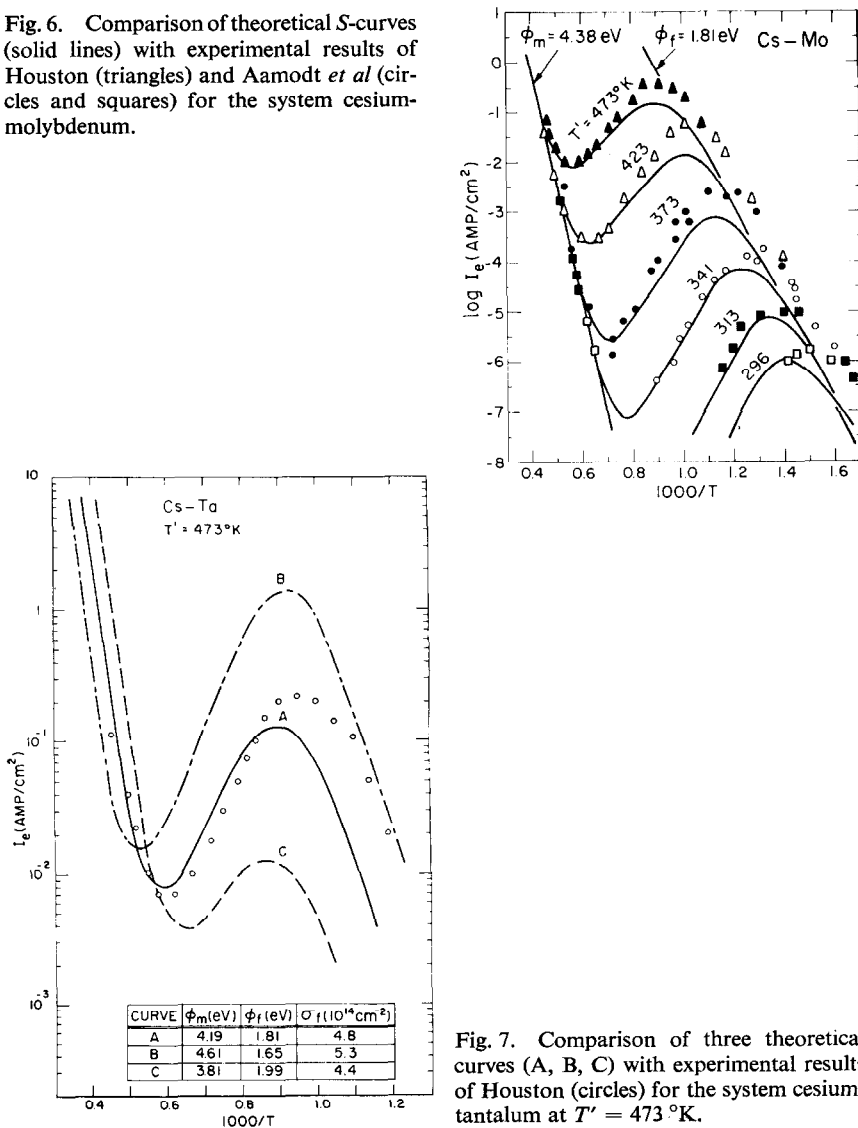


Fig. 7. Comparison of three theoretical curves (A, B, C) with experimental results of Houston (circles) for the system cesium-tantalum at $T' = 473\text{°K}$.

substantiates the selected value $\phi_m = 4.38\text{eV}$ and it could be improved by properly adjusting the values of ϕ_f and σ_f that were not reported.

3.2.3. Cs on polycrystalline Ta

Fig. 7 presents theoretical curves for cesium on tantalum derived for different combinations of ϕ_m , ϕ_f , and σ_f and $T' = 473^\circ\text{K}$. Superimposed on the same figure are data reported by Houston¹⁴⁾ who did not determine ϕ_m , ϕ_f and σ_f . It is estimated that the data can be best approximated by the parameters $\phi_m = 4.19\text{eV}$, $\phi_f = 1.65$ and $\sigma_f = 4.2 \times 10^{14}\text{cm}^{-2}$.

3.2.4. Cs on polycrystalline Nb

Fig. 8 presents theoretically derived S-curves for cesium on niobium and reported experimental data.^{13,14)}* The agreement between theory and experiment is poor even though a variety of combinations of values ϕ_m , ϕ_f and σ_f are used. In order to match the data an unusually low value of $\sigma_f (< 3 \times 10^{14}\text{cm}^{-2})$ must be assumed. This value, however, is surprising since the lattice constants of Nb, W, Mo and Ta are similar.

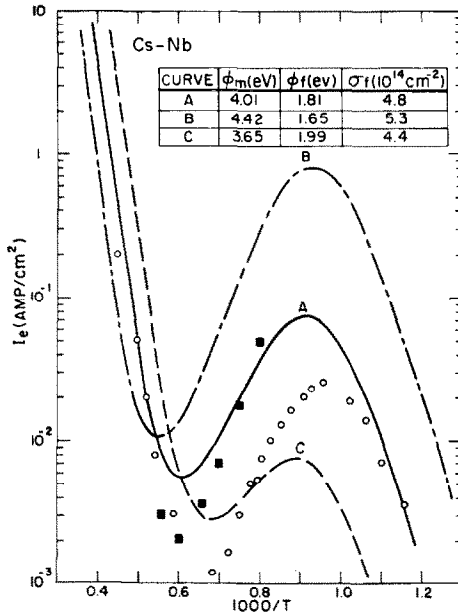


Fig. 8. Comparison of three theoretical curves (A, B, C) with experimental results of Houston (circles) and Hatsopoulos and Kitrilakis (squares) for the system cesium-niobium at $T' = 473^\circ\text{K}$.

* In fig. 7 of ref. 13) "Nb" should be substituted for "Mo". S. Kitrilakis, personal communication.

3.3. PREDICTION OF *S*-CURVES FOR Cs ON OTHER METALS

For completeness and because cesium is frequently used in thermionic energy conversion, some important values of *S*-curves for cesium on 21 transition metals have been calculated. These values are derived for $T' = 573^\circ\text{K}$, typical bare metal electron work functions, ϕ_m , taken from table 1 of ref.²⁾, $\phi_f = 1.81\text{ eV}$ and $\sigma_f = 4.8 \times 10^{14}\text{ cm}^{-2}$. The results are shown in table 1. For each substrate, the emission minimum, the emission maximum, the minimum work function and the surface temperature at which they occur are given.

The table indicates that the emission from the first transition metal series is in an order of magnitude lower than that of the other metals. This is primarily due to the relatively small heat of sublimation of these metals (see also ref.²⁾).

The results also allow the classification of the transition metals either in terms of decreasing minimum emission (W, Re, Mo, Ta, Tc, Nb etc.) or in terms of decreasing maximum emission (W, Re, Mo, Ta, Tc, Nb etc.). The latter classification has also been verified experimentally¹⁴⁾. Admittedly, however, changes in the apparent crystallographic structure of the surface

TABLE 1
Calculated *S*-curve properties for Cs on 21 transition metals at $T' = 200^\circ\text{C}$

Metal	Emission min.		Emission max.		ϕ_e min.	
	(A/cm ²)	(1000/T)	(A/cm ²)	(1000/T)	(eV)	(1000/T)
Ti	6×10^{-5}	0.74	5×10^{-4}	1.07	1.78	1.58
V	2×10^{-4}	0.69	12×10^{-4}	1.01	1.79	1.50
Cr	1×10^{-4}	0.63	6×10^{-4}	1.00	1.79	1.70
Mn	3×10^{-7}	0.96	5×10^{-7}	1.25	1.80	2.02
Fe	3×10^{-4}	0.75	1×10^{-4}	1.07	1.79	1.66
Co	4×10^{-5}	0.75	2×10^{-4}	1.07	1.79	1.64
Ni	1×10^{-5}	0.66	2×10^{-4}	1.01	1.79	1.78
Zr	0.001	0.64	0.01	1.00	1.76	1.29
Nb	0.005	0.62	0.07	0.93	1.78	1.18
Mo	0.008	0.56	0.14	0.88	1.78	1.23
Tc	0.007	0.57	0.11	0.89	1.78	1.24
Ru	0.004	0.57	0.05	0.91	1.78	1.27
Rh	0.002	0.55	0.03	0.93	1.78	1.32
Po	4×10^{-5}	0.68	2×10^{-4}	1.05	1.77	1.68
Hf	0.005	0.68	0.04	0.94	1.78	1.22
Ta	0.008	0.59	0.13	0.90	1.78	1.15
W	0.013	0.54	0.27	0.85	1.77	1.19
Re	0.009	0.50	0.15	0.85	1.77	1.22
Os	0.002	0.50	0.02	0.95	1.78	1.46
Ir	0.002	0.51	0.02	0.92	1.77	1.35
Pt	0.004	0.50	0.05	0.90	1.77	1.30

may overshadow the above results which are derived on the basis of the arbitrarily assumed values of ϕ_m , ϕ_f , σ_f (see also fig. 4).

It is interesting to note that a practically identical classification of the transition metals with regard to maximum emission has been derived by approximating the state equation (eq. 2) by $\phi_a = \phi' T/T'$. The controlling factor of this classification³⁾ is the ratio ϕ_{a0}/ϕ_m where ϕ_{a0} is the atom desorption energy at zero coverage. It is evident from this approximate treatment, as well as from the preceding more accurate analysis, that emitter materials with the higher ϕ_m do not necessarily have the higher emission.

Another result evident from table 1 is that the minimum electron work function is not very different from bulk cesium for all the transition metals. Many experimenters have reported minimum work functions as low as 1.4eV. It is felt that such low values result from contamination of the surface by electronegative contaminants. It is well known for example that traces of oxygen²¹⁾ and fluorine¹⁵⁾ lower the minimum work function in the cesium-metal system. Also, it is experimentally established that the system barium-tungsten has a pronounced minimum²²⁾ which disappears when both clean barium and a clean tungsten surface are used.^{23, 24)}

Finally, the derived values for Ni are in poor agreement with experimental results. Experimentally²⁵⁾ it is found that Ni in the presence of Cs is a good electron emitter even though table 1 classifies it as a poor emitter. But this may be due to contamination.

It is possible to derive *S*-curves for any combination of substrate and adsorbate materials and a given vapor bath temperature. A general computer program is available for this type of parametric study.

Acknowledgements

The authors are indebted to Dr. K. G. Hernqvist and Mr. J. O'Neill, Jr. for the development of the computer program.

References

- 1) E. P. Gyftopoulos and J. D. Levine, *J. Appl. Phys.* **33** (1962) 67.
- 2) J. D. Levine and E. P. Gyftopoulos, *Surface Science* **1** (1964) 171.
- 3) J. D. Levine and E. P. Gyftopoulos, *Surface Science* **1** (1964) 225; a brief summary of ref.¹⁻³⁾ is given by the authors in the 23rd. Ann. Conf. on Phys. Elec., MIT, 239 (March 1963).
- 4) J. H. de Boer, *Advances in Catalysis VIII* (Academic Press, N.Y. 1956) p. 85.
- 5) P. H. Emmett, ed. *Catalysis I and II* (Reinhold Publ. Corp., N.Y., 1954).
- 6) N. S. Razor and C. Warner III, *Atomics Intern. First Summary Report of Basic Research in Thermionic Energy Conversion Processes* (November 1961, AI-6799) p. 45; and *J. Appl. Phys.* (to be published 1964).
- 7) J. B. Taylor and I. Langmuir, *Phys. Rev.* **44** (1933) 423.

- 8) W. E. Danforth, *J. Appl. Phys.* **33** (1962) 1972.
- 9) J. Becker, *Advances in Catalysis VII* (Academic Press, N.Y., 1956) p. 85.
- 10) J. D. Levine, Theory of Ion Emission. RCA Technical Report, PTR-1123 (September 1961).
- 11) W. B. Nottingham, *Direct Conversion of Heat to Electricity*. Ed. Kaye and Welsh (J. Wiley & Sons, N.Y., 1960) p. 8-1.
- 12) E. N. Carabateas, *J. Appl. Phys.* **33** (1962) 2698.
- 13) G. N. Hatsopoulos and S. Kitrilakis, 22nd Ann. Conf. on Phys. Elec. MIT, 152 (March 1962).
- 14) J. M. Houston and H. F. Webster, *Advances in Electronics and Electron Physics* 17 (Academic Press, N.Y., 1962) p. 125.
- 15) R. L. Aamodt, J. L. Brown and B. D. Nichols, *J. App. Phys.* **33** (1962) 2080.
- 16) R. J. Zollweg, *Appl. Phys. Lett.* **2** (1963) 27.
- 17) R. Gomer, *Field Emission and Field Ionization*. (Harvard University Press, 1961).
- 18) S. T. Martin, *Phys. Rev.* **60** (1939) 947.
- 19) H. F. Webster, *J. Appl. Phys.* **32** (1961) 1802.
- 20) See Ref.⁹ for summary; for details see J. Levine, *Proc. of Thermionic Specialists Conf.* (Gatlinburg, Tenn., IEEE October, 1963).
- 21) I. Langmuir and K. H. Kingdon, *Proc. Roy. Soc. (Lond.)* **A107** (1925) 61.
- 22) J. Becker, *Trans. Amer. Electrochemical Soc.* **55** (1929) 153.
- 23) A. J. W. Moore and H. W. Allison, *J. Chem. Phys.* **23** (1955) 1609.
- 24) Ya. P. Zingerman and V. A. Ishchuk, *Soviet Physics Solid State* **4** (1963) 1618.
- 25) B. S. Rump, J. F. Bryant and B. L. Gehman, 23rd Ann. Conf. on Phys. Elect. MIT, 232 (March 1963).